Supplementary Materials

S.1. Neonatal Swine Model

One-week-old, healthy female Yorkshire piglets (n=8; Meck Farms, Lancaster, PA) were included in this study. Animals were housed in the Abramson Research Center Large Animal Facility for a maximum of 7 days prior to study with daily care monitoring by a trained Division of Veterinary Resources technician. All animals underwent identical care and study procedures as described.

Anesthesia

On the morning of study, animals were fasted a minimum of 2 hours prior to receiving a pre-medicated intramuscular injection of ketamine (20mg/kg) for comfort followed by weighing and transport to operating room within the same facility. Prior to intubation, piglets were administered 4% inhaled isoflurane in 100% FiO_2 via snout mask until abolishment of response to reflexive pinch stimulus. Animals were then intubated with a 3mm endotracheal tube with in-line capnometer; placement was confirmed by normative end-tidal CO_2 tracings. Subsequently, a maximum of 1.5% inhaled isofluorane was used for maintenance of anesthesia with depth of anesthesia confirmed by heart rate, blood pressure, mandibular jaw tone, and absence of withdrawal response to toe pinch. Ventilator settings were maintained within a peak expiratory pressure of 6cm H_2O, and tidal volumes (8-12 ml/kg) and respiratory rate titrated to maintain end-tidal CO_2 between 38-42 mmHg.

Surgical Preparation

Piglets were initially positioned prone. Then neuromonitoring and rectal and nasopharyngeal temperature probes for guidance of hypothermic therapy were placed and secured. A heating pad and blanket were placed along the dorsum and ventral aspects and were used as needed to maintain normothermia.

Piglets were then positioned supine, neuromonitoring probe placements optimized, and limbs secured. The right femoral artery and vein were exposed and cannulated to permit pressure transduction and vascular access, respectively. Intravenous fentanyl (25-200 μg/kg/min) and dexmetetomidine (0.5-2.0 μg/kg/min) were initiated and titrated as needed for depth of anesthesia. A standard median sternotomy incision was performed, along with thymectomy, pericardiotomy, and exposure of the great vessels for cannulation. Systemic heparin 200 IU/kg was then administered directly into the right atrium. Additional heparin was used as needed to ensure an activated clotting time (ACT) greater than 400 seconds prior to establishment of cardiopulmonary bypass.

Cardiopulmonary Bypass (CPB)

The cardiopulmonary bypass circuit was primed with 200 ml of Plasmalyte and 300 ml of donor swine whole blood added to establish a hematocrit level of 30%. The prime volume was treated with 500 units of heparin, 1 mEq + 5 mEq/kg of sodium bicarbonate, 1mg/kg of Lasix, and 450 mg of calcium gluconate and swept at 0.5L/min for 2 minutes. Circuit lines were connected via two 3/16" x ¼" connectors and de-aired. The ascending aorta and right atrial appendage were cannulated with a 10-Fr arterial cannula and a 20-Fr single stage venous cannula, respectively. Cardiopulmonary bypass flows were steadily increased to target baseline flows of 150 ml/kg/min and continuously monitored via an ultrasonic flow probe affixed to the arterial outflow. The cardiopulmonary bypass heater/cooler unit was used as necessary to stabilize nasopharyngeal temperature at normothermic baseline (37°C) and for all subsequent periods of cooling and warming as described in the following protocol for deep hypothermia.

Deep Hypothermia (DH) Protocol

Therapeutic deep hypothermia (DH) protocol closely mirrored clinical practice at our institution (*see* **Methods**; **Fig. 2**). DH was directed using nasopharyngeal temperature. Following stable normothermia for a minimum of 5 minutes, subjects were cooled to 18°C at an approximate rate of 1°C per minute by maintaining an 8-10°C gradient between the cooling bath and venous return temperature. Subjects remained under DH with continuous perfusion for a total of 40 minutes, at which point rewarming to normothermia occurred at an approximate rate of 1°C per minute.

Arterial and jugular venous blood sampling (0.3 cc of blood per draw), as described (*see* **Methods**; **Fig. 2**), were analyzed for pH, pCO_2 (mmHg), pO_2 (mmHg), Na+ (mmol/L), K+ (mmol/L), Ca++ (mmol/L), glucose (mg/dL), lactate (mmol/L), and hematocrit (%) and derivation of HCO_3- (mmol/L), base excess (mmol/L), and SO_2 (%) using the point-of-care blood gas analyzer (GEM 3000, Instrumentation Laboratory, Blauvelt, NY, USA). Per clinical protocol at the Children's Hospital of Philadelphia (CHOP), blood pH was optimized by pH-stat management during cooling, whereby increased concentrations of carbon dioxide were added to the oxygenator as necessary to maintain a temperature-corrected pCO_2 of 40 mmHg resulting in a blood pH of 7.4; during rewarming and while normothermic, the blood pH was optimized by alpha-stat (*i.e.*, maintenance of pCO_2 at 40 mmHg without temperature correction).

Mean arterial pressure was maintained between 40-70 mmHg with titration of intravenous nitroglycerin (0.25-20 μg/kg/min), milrinone (50 μg/kg bolus, 0.25-0.75 μg/kg/min infusion), or nicardipine (0.5-3.0 μg/kg/min) as necessary for hypertension. Significant changes in blood pressure, blood gas analytes, hyperglycemic status and any evidence of subject discomfort were treated immediately. At the conclusion of the study, animals were euthanized using 20 mEq/kg of potassium chloride.

S.2. Derivation and Interpretation of Q_{10}

The *temperature coefficient*, Q_{10}, can be expressed as:

$$Q_{10} = \left(\frac{CMRO_{2,1}}{CMRO_{2,2}}\right)^{\frac{10}{T_1 - T_2}}. \quad \text{(S1)}$$

Calculation of Q_{10} requires only two measurement points (*i.e.*, knowledge of a temperature change and corresponding relative change in $CMRO_2$), and intuitively it describes the relative impact of temperature change on metabolism. This scalar coefficient formulation can be directly derived from the definite integral of the van't Hoff Equation or from simple substitution per the Arrhenius Equation. By the Arrhenius Equation,

$$k = Ae^{-\frac{E_a}{RT}}, \quad \text{(S2)}$$

a rate of reaction (k) depends on temperature (T), the universal gas constant (R), an activation free energy barrier (E_a), and a pre-exponential factor (A) which is related to the frequency (*i.e.*, incidence) of reaction. Using $CMRO_2$ as the rate of reaction (k), the relationship between the measured $CMRO_2$ at two different temperatures, T_1 and T_2, is easily shown to be exponentially related to the product of a scalar constant (E_a/R) and the difference of the inverse of the two temperatures:

$$\frac{CMRO_{2,1}}{CMRO_{2,2}} = e^{-\frac{E_a}{R}\left(\frac{1}{T_1} - \frac{1}{T_2}\right)}. \quad \text{(S3)}$$

Simple algebraic rearrangement yields the following expression incorporating the constants E_a, R, and the temperatures, T_1 and T_2:

$$Q_{10} = e^{\frac{E_a}{R}\left(\frac{10}{T_1 T_2}\right)}. \quad \text{(S4)}$$

Assuming a metabolic system is accurately modeled by the Arrhenius equation, this result implies that Q_{10} may be interpreted as a scalar constant, as long as the temperature difference between T_1 and T_2 is relatively small compared to the absolute baseline temperature, T_1, in Kelvin (*i.e.*, $|T_1 - T_2| \ll T_1$ such that $\frac{1}{T_1 T_2} \approx \frac{1}{T_1^2}$). These are reasonable assumptions for studies of cerebral metabolism given the narrow range of normative baseline body temperatures [83]. As a result, even without measurement of absolute metabolism, comparison of the Q_{10} between such studies provides direct insight regarding differences in activation energy E_a of each respective metabolic system.

S.3. Example Cerebral Hemodynamic Time-Series Data

Non-invasive frequency-domain diffuse optical spectroscopy (FD DOS) and diffuse correlation spectroscopy (DCS) enables concurrent and continuous measurement of cerebral hemodynamics and metabolism. A case example of these measurements in

shown in **Figure S1** with corresponding nasopharyngeal temperature (NPT) during induction of deep hypothermia, continuous deep hypothermic perfusion, and rewarming back to normothermia.

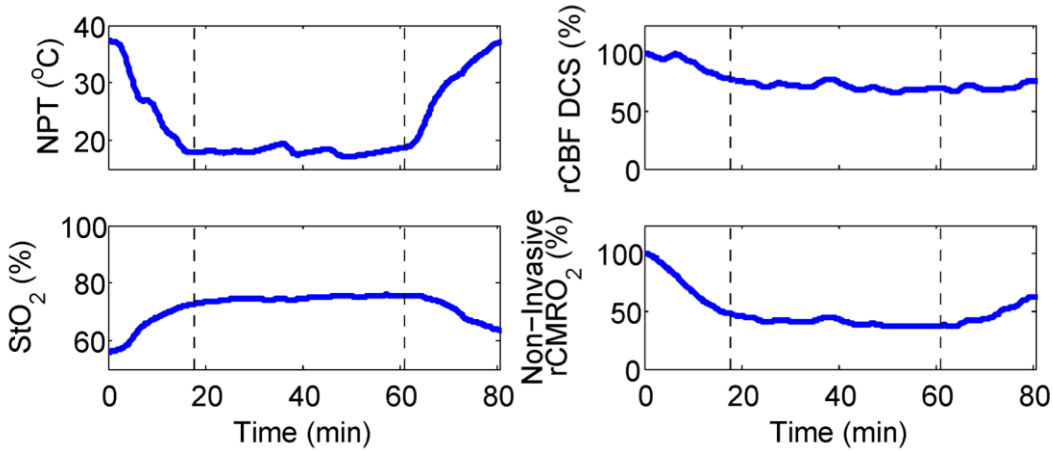

Figure S1: Continuous Cerebral Hemodynamics During Deep Hypothermia – Continuous measurements of cerebral tissue oxygen saturation (StO_2, %) measured using FD DOS, relative cerebral blood flow (rCBF) measured using DCS, and the combined measure of relative cerebral metabolic rate of oxygen ($rCMRO_2$) during cooling, forty minutes of continuous deep hypothermic perfusion, and rewarming. Decrease in temperature causes an increase in StO_2, decrease in rCBF, and decrease in $rCMRO_2$.

S.4. Examination of Cerebral Oxygenation

Cerebral tissue oxygen saturation (StO_2) is expected to be higher than cerebral venous oxygen saturation. However, at all blood gas sampling time-points, $SjvO_2$, our invasive surrogate measure of cerebral venous saturation, was consistently higher than non-invasively measured StO_2 **(Tbl. S1)**.

Table S1. Oxygen Saturation Sampling and Calculated OEF

	Cooling Start	Cooling Mid	Cooling End	Rewarm Start	Rewarm Mid	Rewarm End
SaO_2, %	98.9 (3.0)	100.0 (0.0)	100.0 (0.0)	99.9 (0.2)	99.8 (0.4)	98.3 (2.7)
$SjvO_2$, %	74.1 (14.8)	88.3 (6.6)	93.7 (5.7)	97.2 (2.6)	92.0 (4.8)	82.5 (8.5)
StO_2, %	55.7 (4.2)	63.3 (5.5)	66.1 (8.0)	67.9 (12.3)	62.9 (7.6)	56.4 (6.1)
$eqSbtO_2$, %	11.0 (9.0)	10.8 (3.9)	20.0 (11.3)	37.6 (28.8)	23.9 (29.5)	12.4 (14.3)
$OEF_{optical}$	0.58 (0.06)	0.48 (0.07)	0.44 (0.09)	0.42 (0.16)	0.48 (0.10)	0.57 (0.08)
$OEF_{blood\ gas}$	0.25 (0.15)	0.12 (0.07)	0.06 (0.06)	0.03 (0.03)	0.08 (0.04)	0.16 (0.07)
p-value*	<0.001	<0.001	<0.001	<0.001	<0.001	<0.001

*p-value of two-sample t-test between $OEF_{optical}$ and $OEF_{blood-gas}$

A linear mixed-effects model (**Fig. S2, *left***) was used to quantify the relationship between the repeated measures of $SjvO_2$ and StO_2. A significant ($p<0.001$) and positive slope effect illustrates a strong positive association between the two values; however, the

mean +27.4% bias between the two modalities from Bland-Altman analysis (**Fig. S2, *right***) with the zero-difference line outside the 95% limits of agreement ([+10.5%, +44.4%]) are evidence of a discrepancy from the theoretical compartment model computation of StO_2 (Culver et al., 2003; Ito et al., 2001).

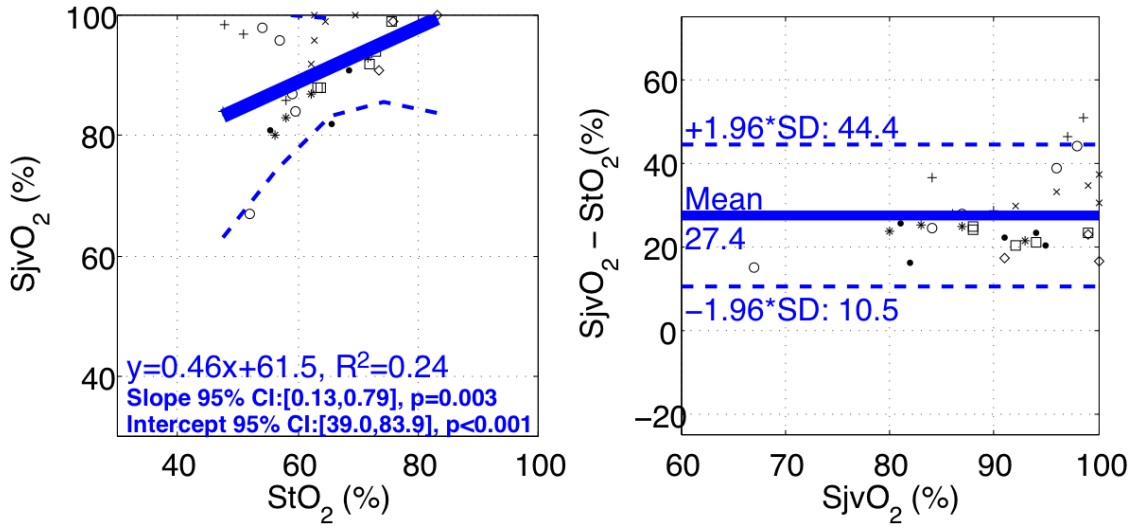

Figure S2: Linear Mixed-Effects Model (*left*) and Bland-Altman Analysis (*right*) of Invasive versus Non-Invasive Oxygen Saturation Measurements – Invasive oxygen saturation derived from jugular venous blood gas sampling ($SjvO_2$) and non-invasive tissue oxygen saturation derived from FD-DOS sampling (StO_2) in n=7 subjects demonstrates a significant (p=0.003) and positive (slope [95% CI] = 0.46 [0.13, 0.79]) association and a bias and precision of +27.4% and 8.7%, respectively.

To further elucidate cerebral oxygen status, our secondary invasive measure of oxygen, $PbtO_2$, was used in combination with invasive intracranial temperature, pH, HCO_3, and base excess, analyzed from corresponding blood gas sampling, to estimate equilibrated vascular saturation of brain tissue ($eqSbtO_2$, %) [89, 90]. This data is listed in **Table S1** and mean and standard deviation plotted alongside non-invasive and invasive saturation data in **Figure S3**). Interestingly, the response to hypothermia and the absolute value of StO_2 during hypothermia is more comparable to $eqSbtO_2$ than the response and absolute value of $SjvO_2$. This observation suggests that non-invasive StO_2 measurements may reflect brain oxygen content better than blood gas sampling from the jugular vein.

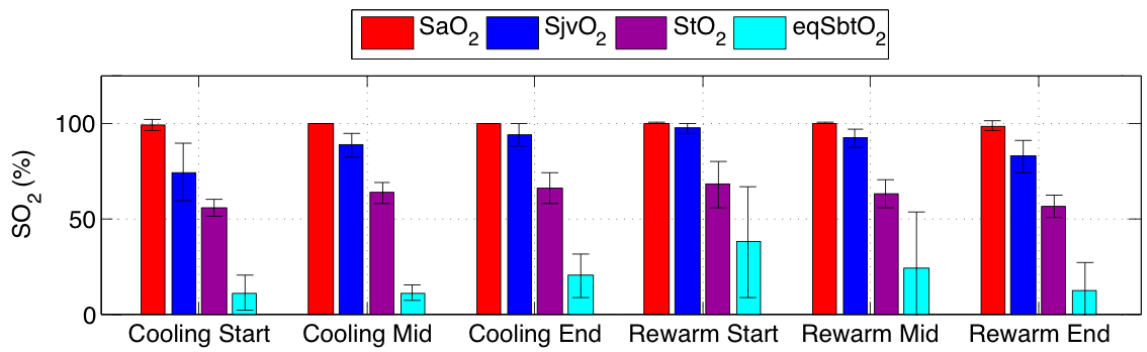

Figure S3: Comparison of Invasive and Non-Invasive Oxygen Saturation Measurements – Mean and standard deviation across subjects (n=7) of oxygen saturation measurements derived from arterial and jugular venous blood gas sampling (SaO_2 and $SjvO_2$, respectively), FD-DOS sampling (StO_2), and invasive $PbtO_2$ measurements ($eqSbtO_2$), are presented for each blood gas sampling time-point.

S.5. Bland-Altman Repeated-Measures Analysis

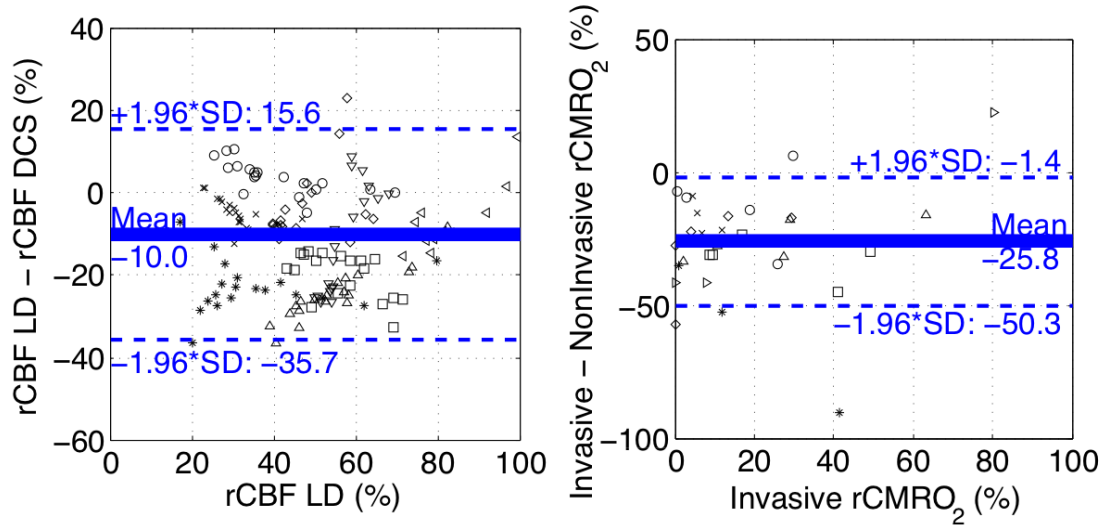

Figure S4: Bland-Altman Analysis of Non-Invasive Diffuse Correlation Spectroscopy (DCS; *left*) and $rCMRO_2$ (*right*) – Data from individual subjects is indicated by a unique symbol. DCS measurements of relative cerebral blood flow (rCBF DCS) demonstrated a mean bias of -10.0% and precision of 13.1% (95% limits of agreement = [-35.7%, 15.6%]) against laser Doppler (rCBF LD; n=8). Non-invasive $rCMRO_2$ quantification demonstrated a mean bias of -25.8% and precision of 12.5% (95% limits of agreement = [-50.3%, -1.4%]) against invasive $rCMRO_2$ measurements (n=7).